CAPE-based derivation of approximate tropical cyclone potential intensity formula

Timothy M. Merlis*

Department of Atmospheric and Oceanic Sciences, McGill University, Montreal, QC, Canada

Raphaël Rousseau-Rizzi

Lorenz Center, Department of Earth and Planetary Sciences, Massachusetts Institute of Technology, Cambridge, MA, USA

Nadir Jeevanjee

NOAA/Geophysical Fluid Dynamics Laboratory, Princeton, NJ, USA

ABSTRACT

Tropical cyclone (TC) potential intensity (PI) theory has been extensively used for future climate change assessments of TC activity. PI theory has a well known approximate form, consistent with a Carnot cycle interpretation of TC energetics, which relates PI to mean environmental conditions: the difference between surface and TC outflow temperatures and the air–sea enthalpy disequilibrium. The changes in these conditions (the increase in air–sea disequilibrium, in particular) provide a physical reason for the robust increase in tropical-mean PI simulated in future climate projections. Quantitative assessments of future changes, in contrast, make use of a numerical algorithm based on the relationship between PI and convective available potential energy (CAPE). Here, a recently developed analytic theory for CAPE is used to present an alternative derivation of an approximate form of PI. The derivation offers insight into the limited sensitivity of PI to the atmospheric stratification in the free troposphere. The resulting CAPE-based approximate formula nearly recovers the previous approximate PI formula, and the new formula helps account for the weaker-than-expected sensitivity of PI to surface relative humidity changes. The new analytic CAPE-based PI builds confidence in previous numerical CAPE-based PI calculations that use climate model projections of the future tropical environment.

1. Introduction

Tropical cyclone (TC) or hurricane potential intensity (PI) theory is the maximum TC intensity that an environment can sustain (Emanuel 1986, 2003). PI is expressed either as a minimum surface pressure or maximum surface windspeed that is determined from the thermodynamic environment. Though most TCs do not reach their PI ($\approx 75\,\mathrm{m\,s^{-1}}$ windspeed in Earth's tropics), PI has been widely used to interpret the climatology, climate variability, and future climate changes of TC activity (e.g., Emanuel et al. 2004; Camargo et al. 2007; Emanuel et al. 2008; Knutson et al. 2010; Sobel et al. 2016).

There have been critiques of PI theory based on its assumptions of axisymmetric TC structure and boundary layer thermodynamics (e.g., Persing and Montgomery 2003; Smith et al. 2008). In spite of these known limitations, PI accounts for the simulated TC intensity increase in TC forecast simulations with warmed temperatures from climate change projections (Knutson and Tuleya 2004) and the sensitivity of TC intensity in single-storm convection permitting simulations to temperature changes (Nolan et al. 2007; Wang et al. 2014). There are also climate-relevant idealized TC simulations (Merlis and Held 2019) with multiple TCs where PI accounts for changes in the TC intensity of the most intense TCs under varied sea surface temperature (Zhou et al. 2014; Merlis et al. 2016). Given these results, it is fair to consider PI a useful perturbation or scaling theory for intensity changes of the most intense TCs. It is PI's temperature sensitivity—where PI has proven useful—that motivates this research, rather than the detailed dynamics of individual TCs—where PI has limitations.

PI has been assessed in future climate warming scenarios by Emanuel (1987) and subsequent generations of climate model simulations have been thoroughly examined (Vecchi and Soden 2007; Sobel and Camargo 2011; Emanuel 2013; Sobel et al. 2016). The tropical-mean PI (assessed over tropical oceans) typically increases in proportion to the tropical surface warming at a rate of $\approx 1\,\mathrm{m\,s^{-1}\,K^{-1}}$. This increase in PI, from a climatological value of $\approx 75\,\mathrm{m\,s^{-1}}$, corresponds to fractional sensitivity of about $1.5\%\,\mathrm{K^{-1}}$. Superimposed on this tropical-mean increase in PI are geographic variations that are substantial in magnitude ($\sim 5\times$ larger than the tropical-mean change with some regional

*Corresponding author: Timothy M. Merlis, timothy.merlis@mcgill.ca

decreases) and uncertain as a result of their dependence on regional climate projections (Vecchi and Soden 2007).

PI theory has a physical interpretation in terms of a Carnot cycle and an approximate formula (described below) that accounts for the tropical-mean PI increase under global warming (Emanuel 1987, 2003; Sobel et al. 2016). However, published assessments of observed PI trends or future climate projections of PI in the recent generations of Coupled Model Intercomparison Project (CMIP) simulations have exclusively made use of an iterative, numerical algorithm for PI that depends on convective available potential energy (CAPE) (Bister and Emanuel 2002). Bister and Emanuel (2002) described the algorithm and a numerical implementation of it has been publicly disseminated by K. Emanuel (`ftp://texmex.mit.edu/pub/emanuel/TCMAX/`). The main reason for introducing the iterative PI algorithm and using it instead of the simpler Carnot formula is that it accounts for the enhancement in surface enthalpy fluxes due to the pressure drop near the center of a mature cyclone, which further strengthens the storm. In addition, if the environment is stable to boundary layer parcels, like in some large-scale subsidence regions, the assumption of environmental moist neutrality in the Carnot-PI formula will cause an overestimation of the intensity achievable by tropical cyclones. The PI algorithm circumvents this problem by removing the assumption of neutrality when the environment is stable. For these reasons, the algorithm PI is more amenable to real-world and comprehensive climate model assessments. The thorough analysis of Garner (2015) describes thermodynamic assumptions made in PI derivations and suggests a 2% discrepancy in the pressure PI climatology when using the publicly released code compared to one that includes the thermodynamic circuit that takes places at pressures below that of the TC (vs. just the circuit between the TC and environmental pressure, see his Fig. 2). Given the importance of PI in scientific and public discourse about climate change's effects on TC intensity, there is a need for a better understanding the relationship between the quantitative analyses that use the publicly disseminated PI-CAPE code and the approximate PI formula, which offers a physical understanding of the origin of the tropical-mean increase in PI under warming. Here, we present a derivation of a new approximate PI formula from the CAPE-based PI that is evaluated analytically using the Romps (2016) theory for CAPE.

This analysis of PI builds on recent research that has made progress in understanding moist convection in the tropical atmosphere by viewing deep convection as an entraining plume that is neutrally buoyant with respect to the environment (Singh and O'Gorman 2013). This line of research has explained the increase in CAPE with warming (Singh and O'Gorman 2013; Seeley and Romps 2015), which is simulated by both cloud-system resolving models and general circulation models (Singh and O'Gorman 2013; Sobel and Camargo 2011). It has also formed the basis of new theories for the relative humidity and thermal stratification of the tropical atmosphere (Romps 2014, 2016). Romps (2016) gives an approximate form of CAPE that can be evaluated analytically. In what follows, this CAPE theory is used to derive an approximate PI formula. For Earth-like conditions, the newly derived CAPE-based PI formula is nearly identical to a well-known earlier formula that makes an analogy between TCs' energetic cycle and that of a Carnot cycle.

We review PI in section 2, derive a CAPE-based approximate PI formula in section 3, compare the CAPE-based PI to the results of numerical CAPE-PI algorithm in section 4, and conclude in section 5.

2. Potential Intensity

a. Approximate form: Carnot cycle

Before presenting the new approximate PI derived from CAPE, the existing approximate form is reviewed. The PI theory developed by Emanuel (1986) assumes axisymmetric structure, angular momentum conserving flow away from the boundary layer, and a well-mixed boundary layer. Here only velocity PI V_{PI} is considered, though results can be translated to pressure PI with a suitable TC structure model (e.g., Chavas et al. 2017).

The approximate formula that has the Carnot engine interpretation, where there is an isothermal enthalpy increase $\propto k_s^* - k_a$ at the warm sea surface temperature T_s, adiabatic expansion in the ascent of the TC eyewall, isothermal enthalpy loss at the cold outflow temperature T_o near the tropopause, and adiabatic compression to the surface, resulting in the following equation (Emanuel 2003):

$$V_{PI}^2 \approx \frac{c_k}{c_d}\frac{T_s - T_o}{T_o}(k_s^* - k_a), \tag{1}$$

with surface (skin) temperature T_s, TC outflow temperature T_o, moist enthalpy $k = c_p T + Lr$, drag coefficient for enthalpy c_k, and drag coefficient for momentum c_d. In the moist enthalpy definition, c_p is the heat capacity at constant pressure of dry air, L is the latent heat of vaporization, and r is the water vapor mixing ratio. The moist enthalpy difference is between the saturated, indicated by *, sea surface $k_s^* = c_p T_s + L r^*(T_s)$ and the surface air $k_a = c_p T_a + L r_a$, where we have neglected the contribution of water vapor to heat capacity. The factor $(T_s - T_o)/T_o$ is often described as a Carnot or thermodynamic efficiency, and the temperature in the denominator depends on whether dissipative heating is recycled (Bister and Emanuel 1998) or not (Emanuel 1986). Here V_{PI} bounds the maximum magnitude of the surface winds. We note that an exact derivation of Eq.1 was provided by Bister and Emanuel (1998), albeit with a different interpretation that does not require the full secondary circulation to correspond to a Carnot cycle.

To estimate the climatological PI, the air–sea enthalpy disequilibrium can be approximated as follows,

$$V_{PI}^2 \approx \frac{c_k}{c_d}\frac{T_s - T_o}{T_o} L r^*(T_s)(1-\mathcal{H}_s),$$

with surface relative humidity $\mathcal{H}_s$ and where the air–sea temperature difference is assumed to be small, an adequate approximation for Earth's tropics. Using representative values of $T_s = 300\,\mathrm{K}$, $T_o = 200\,\mathrm{K}$, equal drag coefficients $c_k/c_d = 1$, $L = 2.5\times10^6\,\mathrm{J\,kg^{-1}}$, $r^*(T_s) = 2.3\times10^{-2}$, and $\mathcal{H}_s = 0.8$, the velocity PI is $\approx 76\,\mathrm{m\,s^{-1}}$. This is similar to the values found using the CAPE-based PI algorithm (section 2b) for Earth's tropics in reanalyses and radiosonde soundings (Bister and Emanuel 2002; Emanuel et al. 2013; Wing et al. 2015; Sobel et al. 2016). Relative humidity only enters this form of the Carnot PI through the thermodynamic disequilibrium term. The first PI derivation introduced by Emanuel (1986), which assumes gradient wind balance above the boundary layer, provides a bound on the azimuthal wind at the top of the boundary layer. In that formulation, T_s in the numerator of the thermodynamic efficiency becomes T_{LCL}, the temperature at the lifting condensation level (LCL). This introduces an additional dependence on boundary layer relative humidity, but the formula is otherwise identical.

Though there has been substantial discussion of upper troposphere and lower stratosphere temperature changes—affecting T_o—on PI (Emanuel et al. 2013; Vecchi et al. 2013), these changes do not dominate the observed trends in recent decades (Wing et al. 2015). Rather, the air–sea disequilibrium increase with warming largely accounts for the tropical-mean PI increase.

The air–sea disequilibrium is related to the surface energy balance because the turbulent surface enthalpy fluxes depend on this disequilibrium. The surface energy budget at equilibrium is:

$$0 = F_{rad} + F_{ocean} - c_k\rho_a|\mathbf{v}|(k_s^* - k_a),$$

with net surface radiation F_{rad} and ocean heat flux convergence F_{ocean}, air density ρ_a, and surface windspeed $|\mathbf{v}|$, where the drag coefficients for latent and sensible turbulent fluxes, c_k, are assumed equal. From this budget, it is clear that the turbulent surface fluxes are constrained by the sum of the net radiation at the surface and ocean heat flux convergence. These can then replace the air–sea enthalpy disequilibrium in the PI equation (1) with the appropriate coefficients from the bulk formula (as described by Emanuel 2007; Emanuel and Sobel 2013):

$$V_{PI}^2 \approx \frac{T_o - T_s}{T_o}\frac{F_{rad} + F_{ocean}}{c_d\rho_a|\mathbf{v}|}.$$

This formula sheds light on the importance of surface energy balance constraints in PI changes (Emanuel and Sobel 2013; Sobel et al. 2019): absent changes in surface windspeed or ocean heat fluxes, the increase in net surface radiation under climate changes (e.g., O'Gorman et al. 2012; Pendergrass and Hartmann 2014) accounts for PI's order $1\%\,\mathrm{K^{-1}}$ sensitivity. This hydrological cycle sensitivity can also be thought of in terms of the tropospheric energy budget, where the origin of the $\approx 1\%\,\mathrm{K^{-1}}$ change can be understood as a consequence of the deepening of the troposphere's depth in temperature coordinates (Jeevanjee and Romps 2018). These energy budget perspectives also help reveal the origin of forcing agent dependence (e.g., greenhouse gas vs. aerosol) of PI changes (Sobel et al. 2019).

b. CAPE-based PI algorithm

PI is related to CAPE through the line integral around the TC cycle (Bister and Emanuel 2002). The velocity PI is given by the following difference between CAPE of the following two parcels:

$$V_{PI}^2 = \frac{T_s}{T_o}\frac{c_k}{c_d}\left(CAPE^* - CAPE^m\right), \tag{2}$$

with the CAPE of a saturated parcel lifted from T_s at TC eyewall pressure denoted $CAPE^*$ ("saturation CAPE") and a parcel with environmental relative humidity, surface air temperature, and TC eyewall pressure denoted $CAPE^m$ ("radius of maximum winds CAPE").

The algorithm iterates to adjust the parcel pressure used in these two CAPE calculations to that of the TC eyewall, taken to be the pressure PI. Because this pressure change relative to the environment is common to the two CAPEs used to determine the velocity PI, it has a modest $\lesssim 10\%$ effect on V_{PI}, consistent with the PI pressure being $\approx 10\%$ lower than the environmental surface pressure in Earth's tropics. We will neglect this pressure dependence in our derivation (section 3) and numerically assess it in section 4.

This algorithm has been used for all quantitative analyses of PI changes in CMIP GCM simulations of climate change (e.g., Vecchi and Soden 2007; Sobel et al. 2019). Yet, it is not straightforward to identify why (2) increases as the climate warms, in contrast to (1). One of the contributions of this research is to develop this understanding. For example, one might ask if the numerically evaluated (2) increase is related to the tropical environment's projected increase in CAPE (e.g., Sobel and Camargo 2011). Our derivation shows that PI changes determined via the CAPE formula are *not*, in fact, related to environmental stratification changes (see also, Garner 2015, for discussion of the limited role role of environmental CAPE in a given climate).

3. Derivation of approximate PI formula from CAPE

Here, we review the CAPE theory of Romps (2016) and then apply it to derive an approximate PI formula.

a. Review of Romps 2016 CAPE theory

Romps (2016) (hereafter, R16) developed a theory for CAPE based on assuming neutrally buoyant entraining plume, following the approach of Singh and O'Gorman (2013). A key to the R16 CAPE theory is a change of coordinates from integrating the buoyancy ($\propto \Delta T$, neglecting virtual temperature effects) in altitude to integrating the buoyancy ($\propto \Delta z$) in temperature. With the change of coordinates ($\int \Delta T dz \rightarrow \int \Delta z dT$), CAPE is defined as

$$CAPE = \frac{g}{T_{avg}} \int_{T_o}^{T_s} [z_0(T) - z_{env}(T)] dT, \qquad (3)$$

with z_0 being the height of non-entraining cloud and z_{env} being the height for the environment, which depends on entrainment. The buoyancy is computed relative to the tropospheric average temperature $T_{avg} = (T_s + T_o)/2$, an approximation of the theory. T_o in (3) is the tropopause temperature that is assumed to be the same in the isothermal stratosphere above. R16 wrote this as T_{FAT} following the fixed-anvil temperature (FAT) hypothesis (Hartmann and Larson 2002), but T_o is used here for consistency with PI literature's outflow temperature.

Then, R16 expressed $z(T)$ in terms of special functions. These heights are given by the following formula, assuming the surface height is zero:

$$z(T) = z_{dry}(T) + z_q(T),$$

where the first right-hand side term corresponds to the height of a dry atmosphere $z_{dry}(T) = c_p[T(z=0) - T]/g$ and the second term is the height that arises from humidity. This term is proportional to the amount of latent heat that has been released from the LCL to an isotherm T, asymptoting to a height $\propto Lq^*_{LCL}/g$ at cold temperatures when all of the latent heat has been released. Here, q denotes specific humidity.

The height that arises from humidity is given by the following formula:

$$z_q(T) = \frac{L}{g(1+a)} [q^*_{LCL} - q^*(T)] H(T - T_{LCL}), \qquad (4)$$

where H is the Heaviside step function and the non-dimensional parameter a is defined as $a = PE\epsilon/\gamma$, with precipitation efficiency PE (non-dimensional, defined as the ratio of net condensation to gross condensation), fractional entrainment rate ϵ (dimensions of inverse length), and fractional lapse rate of saturation specific humidity $\gamma = -\partial_z \log(q^*)$ (dimensions of inverse length). The theory's saturation specific humidity above the parcel's LCL is

$$q^*(T) = (1+a)\frac{RT_{avg}}{L} W[y e^{-\gamma(T_{LCL} - T)})], \qquad (5)$$

where W is the Lambert W function, constant γ, and constant y are defined as:

$$W(x \exp^x) = x,$$
$$\gamma = \frac{L}{R_v T^2_{avg}} - \frac{c_p}{RT_{avg}},$$
$$y = \frac{Lq^*_{LCL}}{(1+a)RT_{avg}} \exp\left[\frac{Lq^*_{LCL}}{(1+a)RT_{avg}}\right].$$

Note that a given parcel, particularly the hurricane parcel, can reach saturation at a level that is distinct from the environmental LCL. If $a = 0$, a moist pseudo-adiabat is recovered. This constant, which affects the climatological dry stability and CAPE, does not affect the PI formula that we derive below.

There are differences in the formula that we presented above and R16. First, R16 writes the tropospheric average temperature (our T_{avg}) as T_0, but this may be confusing in the PI context because of the PI-theory outflow temperature T_o. Second, we use the symbol γ for the thermodynamic constant defined above; R16 used the symbol f for this constant, but we prefer to avoid possible confusion with the Coriolis parameter. Last, the subcloud layer is ignored in R16, which eliminates the step function from (4) and reduces the LCL quantities to surface quantities ($T_{LCL} \rightarrow T_s$ and $q^*_{LCL} \rightarrow q^*_s$). The inclusion of the subsaturated subcloud layer was not necessary in R16 because it is not important to the temperature dependence of CAPE discussed there. Here, it is retained because of the critical importance of the difference in the humidity of the parcel used to evaluate the two CAPEs in (2) and to recover the non-zero PI of a dry atmosphere with an air–sea surface temperature difference.

b. Evaluation of PI with CAPE theory

Here we substitute (3) into (2) and expand the difference between the hurricane CAPE and the environmental CAPE:

$$V^2_{PI} = \frac{T_s}{T_o}\frac{c_k}{c_d}(CAPE^* - CAPE^m)$$
$$= \frac{T_s}{T_o}\frac{c_k}{c_d}\frac{g}{T_{avg}}\left\{\int_{T_o}^{T_s}[z^*_0(T) - z_{env}(T)]dT - \int_{T_o}^{T_s}[z^m_0(T) - z_{env}(T)]dT\right\}.$$

Clearly, there is a common environmental height $z_{env}(T)$ that can be eliminated (see also, Garner 2015), and this also eliminates a sensitivity to entrainment rate:

$$V_{PI}^2 = \frac{T_s}{T_o}\frac{c_k}{c_d}\frac{g}{T_{avg}}\int_{T_o}^{T_s}[z_0^*(T) - z_0^m(T)]dT. \quad (6)$$

Now, the integrand is the remaining height difference, $\Delta z = z_0^*(T) - z_0^m(T)$, of the two non-entraining ($a = 0$) parcels.

To gain an intuition for the analysis that follows, we plot these heights in Fig. 1 (black lines) for a representative conditions: $T_s = 300\,\mathrm{K}$, $T_a = 299\,\mathrm{K}$, $\mathcal{H}_s = 0.8$, and $T_o = 200\,\mathrm{K}$. The dashed line shows the height of the non-entraining parcel lifted from the environmental surface $\mathcal{H}_s$ and air temperature z_0^m and the solid line shows that of the saturated "hurricane" parcel z_0^*. The differences between these—with solid above dashed, implying positive buoyancy—are nearly vertically uniform in the temperature coordinate above the sub-cloud layer ($T \lesssim 295\,\mathrm{K}$). The moist component of height (4) increases from the surface for the saturated parcel to the environmental LCL (blue solid line in Fig. 1), where the other parcel's moist component of height first becomes non-zero. This implies there is a non-zero subcloud contribution to PI, though the buoyancy above the LCL dominates for Earth-like conditions.

The dry component of the height integrates to $c_p(T_s - T_a)(T_s - T_o)/g$ in (6), and the moist component can be handled as follows. The integral can be split into the broken into components above and below the LCL:

$$\int_{T_o}^{T_s}\Delta z_q dT = \int_{T_{LCL}^m}^{T_s}\Delta z_q dT + \int_{T_o}^{T_{LCL}^m}\Delta z_q dT.$$

Above the LCL, the temperature-dependent $q^*(T)$ terms in (4) nearly exactly cancel, with modest deviations as y and the LCL do differ between the parcels [see (5)]. This leaves a humidity difference constant in temperature $q_s^* - q_{LCL}^*$:

$$\int_{T_o}^{T_{LCL}^m}\Delta z_q dT = \frac{L}{g}(q_s^* - q_a)(T_{LCL}^m - T_o), \quad (7)$$

where we assume the humidity is constant from the surface air q_a to the LCL ($q_{LCL}^* = q_a$). Next, the integrated subcloud buoyancy from humidity $L\Delta q/g$ can be obtained from the following expression (see Appendix for details):

$$\int_{T_{LCL}^m}^{T_s}\Delta q dT = q_s^*(T_s - T_{LCL}^m) - \int_{T_{\mathrm{LCL}}}^{T_s} q^*(T)dT \quad (8)$$

$$= q_s^*(T_s - T_{LCL}^m) - \frac{1}{\gamma}\left[q_s^* - q_{\mathrm{LCL}}^* + \frac{L}{2RT_{\mathrm{avg}}}(q_s^{*2} - q_{\mathrm{LCL}}^{*2})\right]. \quad (9)$$

The full PI expression, after assuming $q_{\mathrm{LCL}}^* = q_a$, is then:

$$V_{PI}^2 = \frac{T_s}{T_o}\frac{c_k}{c_d}\frac{1}{T_{avg}}\left\{c_p(T_s - T_a)(T_s - T_o) + Lq_s^*(T_s - T_o) - Lq_a(T_{LCL}^m - T_o) - \frac{L}{\gamma}\left[q_s^* - q_a + \frac{L}{2RT_{\mathrm{avg}}}(q_s^{*2} - q_a^2)\right]\right\}. \quad (10)$$

This is one of the central contributions of this research: we have used the R16 theory for CAPE and the CAPE-based definition of PI to analytically derive a new approximate PI formula. The resulting expression involves familiar environmental quantities (e.g., T_s, T_a, T_o), as well as thermodynamic quantities embedded in the constant γ and the LCL temperature T_{LCL}.

c. Magnitude of terms

To reconcile this new analytic formula with the existing one, we examine the magnitude of the terms in the expression (10) for Earth-like conditions.

First, the sub-cloud humidity contributions are small compared to those of the free-troposphere (7). This can be quantified by considering the magnitude of an upper bound on the sub-cloud term. Replacing the temperature-dependent saturation specific humidity $q^*(T)$ with that of the LCL, q_{LCL}^*, in the sub-cloud term provides the bound: $\int_{T_{\mathrm{LCL}}}^{T_s}\frac{L}{g}(q_s^* - q^*(T)) \le \int_{T_{\mathrm{LCL}}}^{T_s}\frac{L}{g}(q_s^* - q_{\mathrm{LCL}}^*) = \frac{L}{g}(q_s^* - q_{\mathrm{LCL}}^*)(T_s - T_{\mathrm{LCL}})$. Both the sub-cloud and free-troposphere terms now have a common $L(q^* - q_{\mathrm{LCL}}^*)/g$ that is multiplied by a temperature difference. The ratio of the sub-cloud to the free-troposphere temperature difference is ($T_{\mathrm{LCL}} - T_o$=100 K to $T_s - T_{\mathrm{LCL}}$ = 5 K) about 20. Alternatively, assuming the surface air humidity can be approx-

imated by neglecting the air–sea temperature difference $q_a \approx \mathcal{H}_s q_s^*$ and evaluating a Taylor expansion of q_s^* in (9) yields a similar result.

For the Earth-like regime with a negligible sub-cloud contribution, the new PI expression is

$$V_{PI}^2 \approx \frac{T_s}{T_o}\frac{c_k}{c_d}\frac{1}{T_{avg}}\left[c_p(T_s-T_a)(T_s-T_o)+Lq_s^*(T_{LCL}^m-T_o)-Lq_a(T_{LCL}^m-T_o)\right].$$

If the T_{LCL}^m is close to T_s, it becomes

$$V_{PI}^2 = \frac{c_k}{c_d}\frac{T_s-T_o}{T_o}(k_s^*-k_a)\frac{T_s}{T_{avg}}. \qquad (11)$$

This series of approximations illustrates a form of the new PI expression that is nearly identical to (1) can be obtained. The additional factor of T_s/T_{avg} is ≈ 1.2 for Earth-like tropical values. This factor increases the climatological estimate of PI by 10% and would not substantially affect PI's temperature sensitivity.

The appearance of T_{avg}^{-1} in the CAPE-based PI formula that we present here arises from the R16 theory approximation of computing buoyancy relative to the tropospheric average temperature. If the buoyancy is instead computed relative to a density of surface temperature air [i.e., $T_{avg} \to T_s$ in (3)], the above (11) would be identical to the PI Carnot formula (1). However, Seeley and Romps (2015) shows that buoyancy is large in the upper troposphere and this can be understood from a zero-buoyancy entraining plume model and moist thermodynamics. In essence, the additional moist static energy of the undilute parcel is manifest as temperature—and therefore buoyancy—where the temperature is sufficiently cold, in the upper troposphere. As a result, we do not think there is a well justified physical basis to alter the definition of CAPE used at the outset of our derivation to force the resulting PI expression to better conform to previous formula.

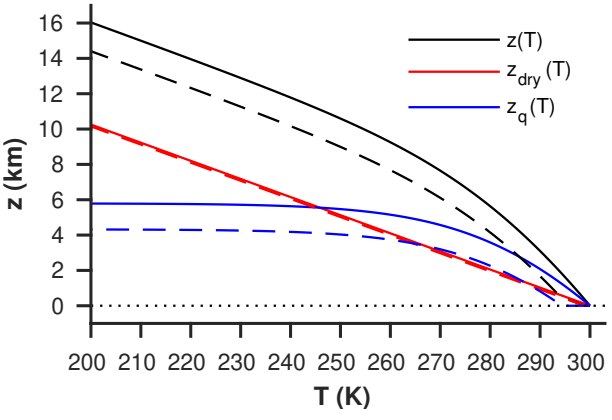

FIG. 1. Height and its components [dry in red and humidity in blue (4)] vs. temperature for the two non-entraining parcels that determine the potential intensity (6) for representative values of relative humidity, surface, surface air, and outflow temperatures. Potential intensity is proportional to the integral of the difference between the black solid and dashed curves.

The fact that moist static energy differences between parcels manifest as buoyancy differences in the upper troposphere also provides intuition for the connection between CAPE-PI and Carnot PI. The air-surface disequilibrium in the Carnot formula (1) is nearly identical to the moist static energy (MSE, $h = c_p T + gz + Lq$, with standard variable definitions) difference between the saturated "hurricane parcel" and environmental parcel. This MSE difference Δh between parcels manifest as buoyancy differences in the mid and upper troposphere. Thus the differences between CAPE in (2) are a vertical integral of this buoyancy ($\propto \Delta h$) difference. Integrating in temperature coordinates is mathematically helpful (details in R16), with the result that the CAPE difference is just the parcel's MSE difference times the temperature depth of the troposphere, normalized by the average tropospheric temperature T_{avg}.

4. Comparison to CAPE-based PI algorithm

In this section, the CAPE-based PI algorithm and derivation are compared using environmental soundings from R16 (i.e., based on the zero-buoyancy entraining plume theory), as a simple representation for a tropical sounding. This is akin to using a moist adiabat as an approximation to a tropical sounding, but includes entrainment. First, we use a representative Earth-like tropical sounding in the PI algorithm to assess the quantitative importance of factors neglected in the derivation of the new analytic formula. Second, we consider a range of soundings with varying surface relative humidity, as a climate variation that possibly distinguishes the new approximate PI formula Eqn. (10) (with its dependence on LCL and surface temperature) from the Carnot approximation (dependent on surface temperature).

The soundings of R16 are specified by the surface air temperature T_a, the outflow temperature T_o, the surface relative humidity $\mathcal{H}_s$, and the non-dimensional parameter characterizing the effect of entrainment on the temperature stratification a. We chose $T_s = 300\,\mathrm{K}$, $T_a = 299\,\mathrm{K}$, $T_o = 200\,\mathrm{K}$, $\mathcal{H}_s = 0.8$, and $a = 0.2$. This value of a is chosen to emulate the results of cloud-system resolving model simulations of radiative convective equilibrium (Romps 2016). We use the CAPE-based PI algorithm with the pseudo-adiabatic ascent option, equal drag coefficients for

momentum and enthalpy ($c_d = c_k$), dissipative heating included, and no windspeed reduction factor to adjust the gradient balance wind (for which PI provides an upper bound) to that of the surface wind. The Carnot formula relies on the assumption of an isothermal outflow layer. Hence, to ensure a meaningful comparison between the algorithm and the Carnot PI, we add an isothermal tropopause on top of the R16 soundings prior to PI computation.

a. Assessment of derivation's approximations

We compare the results of the standard CAPE-based PI algorithm with altered algorithms that bring the numerical algorithm toward the theory by using the same approximations. For the Earth-like sounding, the CAPE-based PI algorithm has a velocity PI of $94.3\,\mathrm{m\,s^{-1}}$ (Table 1, Standard).

TABLE 1. Results of the numerical CAPE-based PI algorithm (2) for the (top row) velocity PI ($\mathrm{m\,s^{-1}}$) for an Earth-like sounding with $T_s = 300\,\mathrm{K}$ (see sec. 4 for other sounding details) and (bottom row) the percentage increase in velocity PI in response to 1 K surface warming. The columns are variants of the algorithm to assess the magnitude of the approximations used in the derivation of (10), with the full description of the altered algorithms in section 4a.

Standard	No iteration	No virtual effect	Buoy. approx.	All
94.3	91.3	91.4	94.2	89.0
4.1%	3.5%	3.8%	4.0%	3.4%

In the derivation of the new approximate form of PI from the R16 CAPE theory, we did not consider the effect of the TC pressure, which is lower than the environment, on CAPE. In particular, a surface pressure of 10^5 Pa representative of the tropical environment was used. To assess the neglect of the TC pressure drop relative to the environment, we alter the CAPE-based PI algorithm by not iterating the parcel pressure to that of the pressure PI. In the numerical algorithm, we perform a single iteration, so that the parcel pressure of the CAPE calculations is equal to that of the environment. Table 1 shows that this decreases the PI by $\approx 3\%$ (No iteration).

The R16 theory for CAPE neglects the virtual (water vapor) effect on density. To assess the omission of the virtual effect, we alter the buoyancy calculation, replacing virtual temperature with temperature, in the algorithm's CAPE subroutine. Table 1 shows that this decreases the PI by $\approx 3\%$ (No virtual effect).

The R16 theory also assumes that the parcel $_p$ buoyancy can be approximated by the ratio of the temperature difference relative to the environment $_e$ and the tropospheric average temperature: $b \propto (T_p - T_e)/T_{avg}$. The PI algorithm computes CAPE as an integral in pressure, rather than altitude. Therefore, we replace the pressure of the R16 sounding—obtained by hydrostatic integration of the vertically varying temperature—with an approximate pressure that is a hydrostatic integration using the tropospheric average temperature T_{avg}. Table 1 shows that this increases the PI by $\approx 0.1\%$ (Buoyancy approx). When all three approximations are used simultaneously, the PI decreases by $\approx 6\%$ (Table 1, All), suggesting that these are small enough approximations that they add linearly.

Table 1 also shows the percentage change in PI when the surface temperature is warmed by 1 K, holding the surface-to-air temperature difference fixed. One might take this to be a starting point for the magnitude of the sensitivity of PI to global warming; however, energetically consistent climate change simulations typically have decreases in the surface-to-air temperature difference and increases in surface relative humidity (e.g., Richter and Xie 2008), which would reduce the PI increase. The standard algorithm has a 4.1% increase in PI for this simple warming case and all of the algorithms have comparable sensitivities (Table 1, bottom row). This shows that the assumptions used in the derivation are modest not only in terms of the climatological PI, but also for the response to climate perturbations.

In summary, the approximations used in the derivation of (10) modestly alter the PI for Earth-like conditions, when they are used in the numerical CAPE-based PI algorithm. This shows that climatological values of PI can be recovered with the simplifications used in the derivation of the approximate formula from CAPE. Furthermore, the sensitivity to a simple warming case is little changed by these approximations.

b. Application to surface relative humidity changes

The Carnot approximate PI formula (1) and the newly derived CAPE-based approximate PI formula (10) have substantial similarity. For example, the form of the dependence on outflow temperature T_o is the same, and they both are sensitive to changes in air–sea enthalpy disequilibrium $k_s^* - k_a$. Therefore, many climate perturbations, such as changing the surface temperature T_s, outflow temperature T_o (here, we are considering this an environmental property of the tropopause and stratosphere), or surface-to-surface air temperature difference will be similar between the two approximate formulas. For example, the new formula has a $3.5\%\,\mathrm{K^{-1}}$ sensitivity and the Carnot formula has a $3.2\%\,\mathrm{K^{-1}}$ sensitivity for the idealized warming described in previous section. One interesting climate variation that potentially distinguishes the two approximate formula are changes in surface relative humidity $\mathcal{H}_s$.

Surface relative humidity changes will influence the Carnot PI formula (1) solely through the surface–air enthalpy disequilibrium. As described in section 2, it can be approximated for Earth-like conditions as $k_s^* - k_a \approx Lq^*(T_s)(1 - \mathcal{H}_s)$. This implies that PI decreases with increased relative humidity following $1 - \mathcal{H}_s$, though neglecting the air–sea temperature difference is not quantitatively

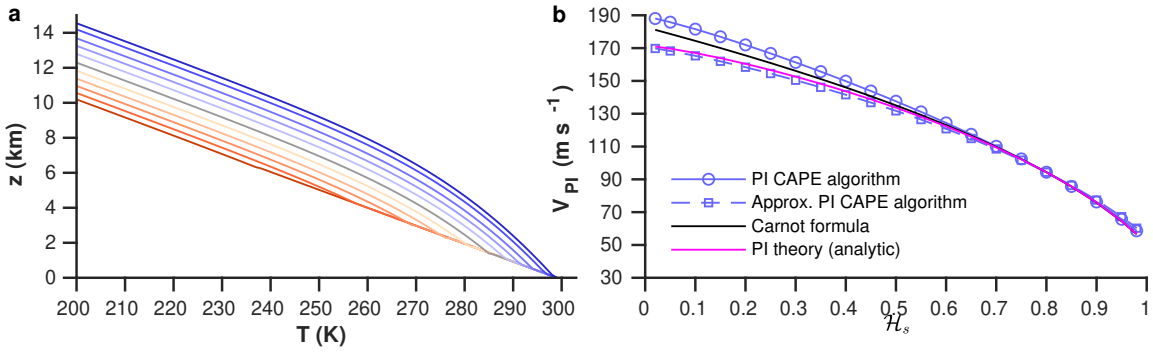

FIG. 2. (a) Temperature vs. height over a range of surface relative humidities with $\mathcal{H}_s = 0.5$ in gray, lower $\mathcal{H}_s$ in successively darker reds, and higher $\mathcal{H}_s$ in successively darker blues. The temperature soundings are shown for the nine integer multiples of $\mathcal{H}_s = N \times 0.1$ and $\mathcal{H}_s = 0.02, 0.98$. (b) Velocity potential intensity vs. surface relative humidity for the numerical CAPE algorithm (2) shown with blue circles, the numerical CAPE algorithm (2) without iterations or virtual effects shown with blue squares (scaling coefficient 1.06), the approximate Carnot formula (1) shown by the black line (scaling coefficient 1.06) and the new analytic formula (10) shown by the magenta line (scaling coefficient 1.02). Additional values of $\mathcal{H}_s$ are shown in (b), as indicated by circles.

accurate for near-saturation conditions. The CAPE-based approximate formula (10) has an additional dependence on the surface relative humidity through the LCL saturation specific humidity q^*_{LCL}, which in turn depends on the LCL temperature. As the relative humidity increases, the LCL temperature increases toward the surface temperature T_s, which *increases* PI relative to the case where changes in LCL temperature are ignored. This sensitivity to relative humidity that arises through the LCL temperature, therefore, offsets part of the sensitivity from the enthalpy disequilibrium term. Here, we compare the approximate formulas to the CAPE-based PI algorithm for a series of soundings generated by varying the surface relative humidity.

Figure 2a shows temperature vs. height for a series of surface relative humidity varying from 0.02 to 0.98 (all other parameters constant with the parameter values described above). The lowest relative humidity (darkest red) produces a sounding similar to a dry adiabat, while the highest relative humidity (darkest blue) has a lapse rate that is affected by latent heat release (more stable) essentially from the surface. It is possible to discern the LCL for intermediate surface relative humidities (Fig. 2a), and it rises in altitude and decreases in temperature as the surface relative humidity decreases. This, according to the new approximate PI formula, would decrease the PI relative to the Carnot formula.

The CAPE-based PI algorithm varies from velocity PI near $190\,\mathrm{m\,s^{-1}}$ to $55\,\mathrm{m\,s^{-1}}$ across this range of soundings (Fig. 2b, blue circles). Taking the Earth-like $\mathcal{H}_s = 0.8$ to be the reference case, the Carnot PI is 6% smaller than the algorithm, and the new formula is only 2% smaller. We suggest that the new approximate formula's closer quantitative agreement in absolute value to the numerical algorithm arises in large part from the previously mentioned factor of T_s/T_{avg} that the Carnot formula does not have. Furthermore, we believe it is likely that the discrepancy in PI absolute value between the CAPE algorithm and Carnot formula has not previously been identified because of other possible differences, such as what pressure to evaluate the air–sea enthalpy differences in (1).

To focus on the sensitivities of the approximate forms of PI relative to that of the CAPE-based algorithm as is relevant for the 'scaling theory' use of PI, we multiply each by a scaling factor to ensure they have the same PI at $\mathcal{H}_s = 0.8$. The Carnot formula has a weaker sensitivity than the algorithm (Fig. 2b, black line vs. blue circles). Figure 2b shows that the new approximate formula (magenta line) is quite similar to the CAPE-based PI algorithm with the same approximations (blue squares), and both of these have weaker sensitivity than the standard CAPE-based PI algorithm (blue circles) and the Carnot formula (black line). That is, it is too insensitive, but properly captures the PI variations aside from those that are explicitly neglected in the derivation. It bears mentioning that the differences are modest for the Earth-like regime of relative humidity $\gtrsim 0.7$.

We note that Cronin and Chavas (2019) found that the results of cloud-system resolving model simulations had PIs for drier simulations similar to or smaller than the PI of saturated surface simulations, using an approximate PI similar to the Carnot formula. The results here are not directly comparable because we simply impose a surface relative humidity change leaving the effect of convective dynamics (encapsulated in the a parameter) and surface-to-air temperature difference unchanged, neither of which would be unchanged with surface drying in convection-permitting simulations.

In summary, the Carnot formula slightly underestimates the sensitivity to an idealized surface drying compared to the numerical CAPE-based algorithm. The new approximation has a somewhat larger deviation from the numerical

CAPE-based algorithm's sensitivity; however, these difference arise from factors neglected in the derivation, as the numerical evaluation of the CAPE algorithm with the same approximations is quite similar to the new analytic formula. Nevertheless, these differences only emerge for fairly dry surfaces, rather than in Earth-like situations.

5. Conclusions

Potential intensity (PI) theory plays an important role in climate change discourse about tropical cyclones (e.g., Sobel et al. 2016). For example, there is confidence in the expectation that the intensity of the most intense tropical cyclones will increase as a result of warming because it is found in both simulations (e.g., Knutson and Tuleya 2004) and PI theory (Emanuel 1987). As such, it is valuable to understand the origin of the tropical-mean increase in PI, upon which the strong, but model-dependent spatial variations are superimposed. The tropical-mean PI increase is robustly simulated and has previously been interpreted in terms of the Carnot-cycle based approximate PI formula that depends on the air–sea enthalpy disequilibrium, which increases with warming. However, quantitative assessments of PI changes in climate models use the iterative numerical CAPE-based algorithm, where it is less clear why PI increases with warming.

Here, a new analysis of PI is presented. We use the CAPE-based definition of PI, which has been the basis for quantitative assessments of PI in future climate change projections using the CAPE-based PI algorithm (Bister and Emanuel 2002). The CAPE-based definition of PI is evaluated here using analytic formula for CAPE from on the theory of Romps (2016). The resulting approximate PI formula and its sensitivity to warming are comparable to the previously discussed approximate Carnot form of PI, though the new formula's PI is $\approx 10\%$ higher. The derivation uses approximations that lead to modest $\lesssim 5\%$ changes when the CAPE-based algorithm is modified to use the same approximations (Table 1), suggesting no quantitatively important errors are introduced in our derivation of an approximate PI formula.

The derivation and the new approximate formula shed light on what determines PI. First, the reason why PI is insensitive to the free-tropospheric stratification[1] emerges clearly as the result of canceling of the environmental soundings between the two CAPEs that determine velocity PI (6). Second, the new approximate PI formula has a dependence on the LCL temperature in addition to the surface temperature (10), rather than just the surface temperature (1). This underlies why it has more muted PI changes under decreasing surface relative humidity than the Carnot formula, which has a rapid increase as $k^* - k_a$ increases (Fig. 2). There is a non-zero subcloud contribution to the buoyancy that decreases as the relative humidity increases and $q^*_{LCL} \to q^*_s$.

The research presented here connects the numerical CAPE PI algorithm to an approximate formula that is quite similar to the existing Carnot approximate formula. This bridges the gap between the quantitative technique used to assess future climate model projections and the physical explanation for the increase in PI under warming as the result of near-surface thermodynamic changes.

Data availability statement. The code to reproduce the figures is available at `https://web.meteo.mcgill.ca/~tmerlis/code/merlis_etal21_cape_pi_code.tgz`.

Acknowledgments. The authors thank Kerry Emanuel for providing the PI-CAPE code (`ftp://texmex.mit.edu/pub/emanuel/TCMAX/`) and Stephen Garner, Paul O'Gorman, Adam Sobel, and Wenyu Zhou for motivating discussions. TM was supported by a NSERC Discovery grant and Canada Research Chair (Tier 2).

[1]We note that the insensitivity of PI to the tropospheric stratification in PI theory does not necessarily imply that simulated or observed sensitivities of TCs to it is weak (e.g., Kieu and Zhang 2018).

APPENDIX

Derivation of subcloud contribution to PI

For the subcloud-layer contribution to PI, an analytic expression for the integral of humidity can be obtained with the following change of variables:

$$
\begin{aligned}
\int_{T_{\rm LCL}}^{T_s} q^*(T)dT &= (1+a)\frac{RT_{\rm avg}}{L}\int_{T_{\rm LCL}}^{T_s} W(ye^{-\gamma(T_s-T)})dT, \quad \text{now let } u = ye^{-\gamma(T_s-T)},\ dT = \tfrac{1}{\gamma}\tfrac{du}{u} \\
&= (1+a)\frac{RT_{\rm avg}}{L\gamma}\int_{u_{\rm LCL}}^{u_s}\frac{W(u)}{u}du, \qquad \text{now let } v = W(u),\ \tfrac{du}{u} = (1+1/v)dv \\
&= (1+a)\frac{RT_{\rm avg}}{L\gamma}\int_{v_{\rm LCL}}^{v_s}(1+v)dv \\
&= (1+a)\frac{RT_{\rm avg}}{L\gamma}\left(v+\frac{1}{2}v^2\right)\Big|_{v_{\rm LCL}}^{v_s} \\
&= (1+a)\frac{RT_{\rm avg}}{L\gamma}\left[W(y)-W(ye^{-\gamma(T_s-T_{\rm LCL})})+\frac{1}{2}W^2(y)-\frac{1}{2}W^2(ye^{-\gamma(T_s-T_{\rm LCL})})\right] \\
&= \frac{1}{\gamma}\left[q_s^*-q_{\rm LCL}^*+\frac{L}{2(1+a)RT_{\rm avg}}(q_s^{*2}-q_{\rm LCL}^{*2})\right],
\end{aligned}
$$

where the last step uses R16 theory for saturation specific humidity (5). Note that $q^*_{\rm LCL}$ in the last line is really q^* at $T_{\rm LCL}$ along the surface parcel's moist adiabat, and that this adiabat will reach the temperature $T_{\rm LCL}$ at a slightly different pressure than the actual LCL. But for Earth-like relative humidity values this pressure difference is small, and we may approximate this as $q^*_{\rm LCL}$.

References

Bister, M., and K. A. Emanuel, 1998: Dissipative heating and hurricane intensity. *Meteorol. and Atmos. Phys.*, **65**, 233–240.

Bister, M., and K. A. Emanuel, 2002: Low frequency variability of tropical cyclone potential intensity 1. Interannual to interdecadal variability. *J. Geophys. Res.*, **107**, 4801.

Camargo, S. J., K. A. Emanuel, and A. H. Sobel, 2007: Use of a genesis potential index to diagnose ENSO effects on tropical cyclone genesis. *J. Climate*, **20**, 4819–4834.

Chavas, D. R., K. A. Reed, and J. A. Knaff, 2017: Physical understanding of the tropical cyclone wind-pressure relationship. *Nature Communications*, **8**, 1360.

Cronin, T. W., and D. R. Chavas, 2019: Dry and semidry tropical cyclones. *J. Atmospheric Sci.*, **76**, 2193–2212.

Emanuel, K., 2003: Tropical cyclones. *Annu. Rev. Earth. Planet. Sci.*, **31**, 75–104.

Emanuel, K., 2007: Environmental factors affecting tropical cyclone power dissipation. *J. Climate*, **20**, 5497–5509.

Emanuel, K., C. DesAutels, C. Holloway, and R. Korty, 2004: Environmental control of tropical cyclone intensity. *J. Atmos. Sci.*, **61**, 843–858.

Emanuel, K., and A. Sobel, 2013: Response of tropical sea surface temperature, precipitation, and tropical cyclone-related variables to changes in global and local forcing. *J. Adv. Model. Earth Syst.*, **5**, 447–458.

Emanuel, K., S. Solomon, D. Folini, S. Davis, and C. Cagnazzo, 2013: Influence of tropical tropopause layer cooling on Atlantic hurricane activity. *J. Climate*, **26**, 2288–2301.

Emanuel, K., R. Sundararajan, and J. Williams, 2008: Hurricanes and global warming: Results from downscaling IPCC AR4 simulations. *Bull. Am. Meteor. Soc.*, **89**, 347–367.

Emanuel, K. A., 1986: An air-sea interaction theory for tropical cyclones. Part I: Steady-state maintenance. *J. Atmos. Sci.*, **43**, 585–604.

Emanuel, K. A., 1987: The dependence of hurricane intensity on climate. *Nature*, **326**, 483–485.

Emanuel, K. A., 2013: Downscaling CMIP5 climate models shows increased tropical cyclone activity over the 21st century. *Proc. Nat. Acad. Sci.*, **110**, 12 219–12 224.

Garner, S., 2015: The relationship between hurricane potential intensity and CAPE. *J. Atmos. Sci.*, **72**, 141–163.

Hartmann, D. L., and K. Larson, 2002: An important constraint on tropical cloud-climate feedback. *Geophys. Res. Lett.*, **29**, 1951, doi:10.1029/2002GL015835.

Jeevanjee, N., and D. M. Romps, 2018: Mean precipitation change from a deepening troposphere. *Proc. Nat. Acad. Sci.*, **115**, 11 465–11 470.

Kieu, C., and D.-L. Zhang, 2018: The control of environmental stratification on the hurricane maximum potential intensity. *Geophys. Res. Lett.*, **45**, 6272–6280.

Knutson, T. R., and R. E. Tuleya, 2004: Impact of CO_2-induced warming on simulated hurricane intensity and precipitation: Sensitivity to the choice of climate model and convective parameterization. *J. Climate*, **17**, 3477–3495.

Knutson, T. R., and Coauthors, 2010: Tropical cyclones and climate change. *Nat. Geosci.*, **3**, 157–163.

Merlis, T. M., and I. M. Held, 2019: Aquaplanet simulations of tropical cyclones. *Curr. Clim. Change Rep.*, 1–11.

Merlis, T. M., W. Zhou, I. M. Held, and M. Zhao, 2016: Surface temperature dependence of tropical cyclone-permitting simulations in a spherical model with uniform thermal forcing. *Geophys. Res. Lett.*, **43**, 2859–2865.

Nolan, D. S., E. D. Rappin, and K. A. Emanuel, 2007: Tropical cyclogenesis sensitivity to environmental parameters in radiative-convective equilibrium. *Quart. J. Roy. Meteor. Soc.*, **133**, 2085–2107.

O'Gorman, P. A., R. P. Allan, M. P. Byrne, and M. Previdi, 2012: Energetic constraints on precipitation under climate change. *Surv. Geophys.*, **33**, 1–24.

Pendergrass, A. G., and D. L. Hartmann, 2014: The atmospheric energy constraint on global-mean precipitation change. *J. Climate*, **27**, 757–768.

Persing, J., and M. T. Montgomery, 2003: Hurricane superintensity. *J. Atmos. Sci.*, **60**, 2349–2371.

Richter, I., and S.-P. Xie, 2008: Muted precipitation increase in global warming simulations: A surface evaporation perspective. *J. Geophys. Res.*, **113**, D24 118.

Romps, D. M., 2014: An analytical model for tropical relative humidity. *J. Climate*, **27**, 7432–7449.

Romps, D. M., 2016: Clausius-Clapeyron scaling of CAPE from analytical solutions to RCE. *J. Atmos. Sci.*, **73**, 3719–3737.

Seeley, J. T., and D. M. Romps, 2015: Why does tropical convective available potential energy (CAPE) increase with warming? *Geophys. Res. Lett.*, **42**.

Singh, M. S., and P. A. O'Gorman, 2013: Influence of entrainment on the thermal stratification in simulations of radiative-convective equilibrium. *Geophys. Res. Lett.*, **40**, 4398–4403.

Smith, R. K., M. T. Montgomery, and S. Vogl, 2008: A critique of Emanuel's hurricane model and potential intensity theory. *Quart. J. Roy. Meteor. Soc.*, **134**, 551–561.

Sobel, A. H., and S. J. Camargo, 2011: Projected future seasonal changes in tropical summer climate. *J. Climate*, **24**, 473–487.

Sobel, A. H., S. J. Camargo, T. M. Hall, C.-Y. Lee, M. K. Tippett, and A. A. Wing, 2016: Human influence on tropical cyclone intensity. *Science*, **353**, 242–246.

Sobel, A. H., S. J. Camargo, and M. Previdi, 2019: Aerosol versus greenhouse gas effects on tropical cyclone potential intensity and the hydrologic cycle. *J. Climate*, **32 (17)**, 5511–5527.

Vecchi, G. A., S. Fueglistaler, I. M. Held, T. R. Knutson, and M. Zhao, 2013: Impacts of atmospheric temperature trends on tropical cyclone activity. *J. Climate*, **26**, 3877–3891.

Vecchi, G. A., and B. J. Soden, 2007: Increased tropical Atlantic wind shear in model projections of global warming. *Geophys. Res. Lett.*, **34**, L08 702.

Wang, S., S. J. Camargo, A. H. Sobel, and L. M. Polvani, 2014: Impact of the tropopause temperature on the intensity of tropical cyclones: An idealized study using a mesoscale model. *J. Atmos. Sci.*, **71**, 4333–4348.

Wing, A. A., K. Emanuel, and S. Solomon, 2015: On the factors affecting trends and variability in tropical cyclone potential intensity. *Geophys. Res. Lett.*, **42**, 8669–8677.

Zhou, W., I. M. Held, and S. T. Garner, 2014: Parameter study of tropical cyclones in rotating radiative–convective equilibrium with column physics and resolution of a 25-km GCM. *J. Atmos. Sci.*, **71**, 1058–1069.